Structural and EPR Studies of Vanadium Complexes of Deprotonated Amide Ligands: Effects on the ^{51}V Hyperfine Coupling Constant

Charles R. Cornman,* Edward P. Zovinka, Yvette D. Boyajian, Katherine M. Geiser-Bush, Paul D. Boyle, and Phirtu Singh

Department of Chemistry, North Carolina State University, Raleigh, North Carolina 27695-8204

Received December 13, 1994[⊗]

The effect of amide coordination on the parallel coupling constant has been determined for three square pyramidal vanadyl complexes. The complexes $V^{IV}O$(PAAP), $V^{IV}O$(PAIS), and $[V^{V}O(HIBA)][C_4H_9)_4N]$ have been prepared, and the latter two have been structurally characterized (PAAP is the dianion of 1,2-bis(2-carboxamidopyridyl)-benzene, PAIS is the dianion of [*N*-(salicylideneamine)phenyl]pyridine-2-carboxamide], HIBA is the tetraanion of 1,2-bis(2-hydroxy-2-methylpropanamido)benzene). X-ray diffraction quality crystals of $V^{IV}O$(PAIS) were obtained by slow evaporation of a nitromethane solution of $V^{IV}O$(PAIS). X-ray parameters for $V^{IV}O$(PAIS): $C_{19}H_{13}N_3O_3V_1$, 382.08 g/mol, $P2_1/n$, a = 7.777(3) Å, b = 18.433(7) Å, c = 11,565(4) Å, β = 102.66(3)°; V = 1633(1) Å3; Z = 4. The final refinement yielded R = 0.0600 and R_w = 0.0450. X-ray diffraction quality crystals of $[V^{V}O(HIBA)][(C_4H_9)_4N]$ were obtained by slow evaporation of a THF–$CHCl_3$ solution of $[V^{V}O(HIBA)]$-$[(C_4H_9)4N]$. X-ray parameters for $[V^{V}O(HIBA)][C_4H_9)_4N]$: $C_{30}H_{52}N_3O_5V_1$, 585.69 g/mol, $P2_1/n$; a = 13.228(3) Å, b = 16.054(4) Å, c = 14.7140(20) Å, β = 93.240(10)°; V = 3119.7(11) Å^3; Z = 4. The final refinement yielded R = 0.051 and R_w = 0.047. Comparison of calculated and experimental values of $A_{||}$ for vanadyl–bleomycin and vanadyl–serum albumin support the presence of a deprotonated amide donor(s) in vanadyl–bleomycin but not in vanadyl–serum albumin.

Introduction

Vanadium is increasingly recognized as being requisite to biological function, dysfunction, and therapy.[1] Since the discovery by Henze in 1911 of high concentrations of this element in the blood of ascidians,[2] vanadium has been identified as an essential element in an alternative nitrogenase[3] and a haloperoxidase.[4] A vanadium protein has also been proposed to catalyze the oxidation of NADH.[5] The necessity of vanadium to higher plants and animals is now unquestioned, especially with regard to the ability of vanadium to modify phosphate metabolism.[6] Arguably, the most important observation regarding vanadium biochemistry is that *orally administered* vanadium has the ability to induce many of the same effects as insulin in diabetic lab animals and humans. To fully understand the bioinorganic chemistry of this element, it is necessary to characterize the various modes of metal uptake/elimination, transport, and function. Many of these processes will involve association of vanadium(V) or vanadium(IV) with polypeptides and/or proteins. The details of these associations, such as binding constants, acid/base properties, and redox potentials, are defined by the specific ligands coordinated to, and the geometry of, the metal ion. This vanadium coordination chemistry can be probed by ^{51}V NMR for vanadium(V) (d^0, S = 0, I = $^7/_2$) or EPR for vanadium(IV) (d^1, S = $^1/_2$).

In addition to the common ligands derived from amino acid side chains, one must also consider that the heteroatoms of the peptide backbone may also provide donors to the first coordination sphere of vanadium. These include the amino- and carboxylate-terminal groups, amide carbonyl oxygen, and amide nitrogen. Naturally occurring metal–amide complexes are rare; however, this ligand is presumed to be important to the transport of metal ions by serum albumin, to be present in metal complexes of bleomycin[7] and in a high pH form of the blue copper protein stellacyanin.[8] In general, coordination of deprotonated amide nitrogen causes a significant decrease in metal centered redox potentials and it is an amide associated ligand-to-metal charge-transfer that is responsible for the photodecomposition of many copper-amide complexes.[9]

Vanadyl complexes of serum albumin,[10] a carrier of vanadium in blood, and bleomycin,[7] a competent DNA cleavage agent, have been previously examined with the knowledge that the vanadium binding sites might involve deprotonated amide ligands. In the former case, it was concluded that amide nitrogens are not involved in vanadyl coordination.[10] Amide coordination has been inferred for interactions between vanadium(V) and peptides. Rehder has examined the formation of 1:1 vanadium(V)–dipeptide complexes using ^{51}V NMR and has concluded that the terminal amine, deprotonated amide nitrogen,

[⊗] Abstract published in *Advance ACS Abstracts,* June 15, 1995.

(1) For a review of vanadium bioinorganic chemistry, see: (a) Butler, A.; Carrano, C. J. Coordination Chemistry of Vanadium in Biological Systems. *Coord. Chem. Rev.* **1991**, *109*, 61–105. (b) Chasteen, N. D., *Vanadium in Biological Systems*; Kluwer Academic Publishers: Dordrecht, The Netherlands, **1990**.
(2) Henze, M. *Hoppe-Seyler's Z. Physiol. Chem.* **1911**, *72*, 494–501.
(3) Robson, R. L.; Eady, R. R.; Richardson, T. H.; Miller, R. W.; Hawkins, M.; Postgate, J. R. *Nature* **1986**, *322*, 388–390.
(4) Butler, A.; Walker, J. V. *Chem Rev.* **1993**, *93*, 1937–1944.
(5) Coulombe, R. A.; Briskin, D. P.; Keller, R. J.; Thornley, W. R.; Sharma, R. P. *Arch. Biochem. Biophys.* **1987**, *255*, 267–273, and references therein.
(6) Nielsen, H. F.; Uthus, E. O., In *Vanadium in Biological Systems*; Chasteen, N. D., Ed. Kluwer Academic Press: Dordrecht, The Netherlands 1990; pp 51–62.
(7) Kuwahara, J.; Suzuki, T.; Sugiura, Y., *Biochem. Biophys. Res. Commun.* **1985**, *129*, 368–374.
(8) (a) Thomann, H.; Bernardo, M.; Baldwin, M. J.; Lowery, M. D.; Solomon, E. I., *J. Am. Chem. Soc.* **1991**, *113*, 5911–5913. (b) Fields, B. A.; Guss, J. M.; Freeman, H. C. *J. Mol. Biol.* **1991**, *222*, 1053–1065.
(9) (a) Hamburg, A. W.; Margerum, D. W. *Inorg. Chem.* **1983**, *22*, 3884–3893. (b) Lee, G.-H.; Larson, J. L.; Perkins, T. A.; Schanze, K. S. *Inorg. Chem.* **1990**, *29*, 2015–2017 and references therein.
(10) (a) Chasteen, N. D.; Francavilla, J. *J. Phys. Chem.* **1976**, *80*, 867–871. (b) Chasteen, N. D.; Grardy, J. K.; Holloway, C. E. *Inorg. Chem.* **1986**, *25*, 2754–2760.

0020-1669/95/1334-4213$09.00/0

and terminal carboxylate are involved in coordination.[11] The observation that pro−gly (unprotected amide nitrogen) does coordinate to vanadium while gly−pro (protected amide nitrogen) does not coordinate to vanadium certainly supports the proposed amide coordination. To date, only one structurally-characterized vanadium(III)-amide complex[12] and one vanadium(V)−amide complex[13] have been presented. Kabanos and co-workers[12,14] and Raymond and co-workers[15] have prepared several structurally characterized vanadium(IV)−amide complexes.

Electron paramagnetic resonance spectroscopy has often been used to suggest the identity of coordinated ligands based on empirical relationships between spectral parameters (g and A) and the coordination sphere of model complexes.[16] This has been especially valuable for vanadium(IV) complexes where EPR has been used in conjunction with ENDOR and ESEEM to study the metal binding site of many metalloproteins.[17] The parallel component of the hyperfine coupling constant, $A_{||}$, is sensitive to the specific ligands of the *equatorial* coordination sphere and has proven useful in ascertaining the equatorial ligands. The empirical additivity relationship in eq 1 may be

$$A = \sum_i n_i A_i \qquad (1)$$

used to estimate the isotropic (A_0) or anisotropic (A_x, A_y, or A_z) coupling constant. Here, n_i is the number of equatorial ligands of type i and A_i is the contribution from each equatorial ligand of type i.[16] A_i, as defined here, is equivalent to one-fourth the value of A for a complex that has only one type of equatorial donor, *vis.* $V^{IV}O(L_i)_4$.[18] $A_{z,i}$ is the z component of this contribution. An A_z ($A_{||}$) range of 120×10^{-4} cm^{-1} to 180×10^{-4} cm^{-1} is observed in most biological matrices. While A_0, A_x, A_y, or A_z can be used in eq 1, A_z is most sensitive to the equatorial ligands and thus has been the focus of the present study. Additionally, A_z can be determined with good accuracy directly from the spectral data without the need for computer simulation. (In this work, the spectral parameters have been calculated as described in the Experimental Section.) Comparison of the calculated and experimental values of $A_{||}$ can be used to argue for or against the presence of specific ligands.

It should be noted that the values of A_i might be expected to depend on the geometry of the vanadium model complex. While large geometric distortions could cause eq 1 to break down, this has not been directly shown. The non-bonding nature of the spin-containing d_{xy} orbital may significantly decrease this geometric dependence. Because of the non-bonding nature of the d_{xy} orbital, electron spin density at the vanadium nucleus will be more influenced by the *average* electron donation (through any bonding orbitals) than changes in *specific* metal−ligand orbital overlap. Preliminary studies of this dependence suggest small variations in geometry do not have a large effect on A_z.[19] The accuracy of eq 1, which has been estimated to be $\pm 3 \times 10^{-4}$ cm^{-1},[16] may account for small structural differences in the model complexes used to determine the values of A_i.[20] Thus, it is conservative to state that this analysis of A_z can be effective in evaluating the average electron donation of the equatorial coordination sphere and, through this average, the nature of the specific ligands.

In the present work, the influence of amide coordination on A_z has been determined for several square pyramidal complexes. Comparison of calculated and experimental values of A_z for vanadyl−bleomycin and vanadyl−serum albumin support the presence of a deprotonated amide donor(s) in vanadyl−bleomycin but not in vanadyl−serum albumin.

Experimental Section

Materials. Materials were purchased from commercial sources and used as received unless otherwise stated. Dry solvents were prepared by distillation from benzophenone ketyl (THF), $Mg(OMe)_2$ (methanol), or CaH_2 (acetonitrile). Elemental analyses were performed by either Galbraith Laboratories or the Analysis Facility of the University of California, Berkeley.

Synthesis. The ligands H_4HIBA[21] and H_2PAAP[22] were prepared according to literature procedures. H_2PAIS was prepared from the Schiff-base condensation of salicylaldehyde with *N*-(2-aminophenyl)-pyridine-2-carboxamide (pyca).[14] Salicylaldehyde (0.67 g, 5.5 mmol) and pyca (1.0 g, 4.7 mmol) were dissolved in 125 mL of ethanol, and the solution was gently refluxed for 2 h. Cooling to room temperature produced a yellow microcrystalline precipitate that was collected by filtration. Slow evaporation yielded a second crop of crystals. Yield: 0.47 g, 30%. No attempt was made to optimize the yield of this reaction.

$V^{IV}O$(PAAP). H_2PAAP (0.51 g, 1.6 mmol) and oxovanadium(V) triisopropoxide (0.48 g, 1.8 mmol) were placed in 100 mL of methanol, and the mixture was brought to reflux. After 3 h of refluxing, the resultant red slurry was filtered (hot) to yield 0.16 g of orange needles. Yield: 0.25 g, 41%. Anal. Calcd (found): C, 56.41 (56.11); H, 3.16 (3.16); N, 14.62 (14.58); V, 13.29 (12.54).

$V^{IV}O$(PAIS). H_2PAIS (0.13 g, 0.40 mmol) and vanadyl acetylacetonate (0.11g, 0.40 mmol) were placed in 100 mL of methanol, and the slurry was brought to reflux. After overnight refluxing, the solvent was removed from the resulting brown solution under vacuum. The brown residue was recrystallized from hot nitromethane to yield a brown microcrystalline product. Yield: 0.11 g, 71%. Anal. Calcd (found): C, 59.70 (59.60); H, 3.43 (3.59); N, 10.99 (11.10); V, 13.32 (12.99). Diffraction quality crystals were obtained by slow evaporation of a nitromethane solution of $V^{IV}O$(PAIS).

[$(C_4H_9)_4N$][V^VO(HIBA)]. [$(C_4H_9)_4N$][V^VO(HIBA)] was prepared in a manner directly analogous to the potassium salt[13] except [$(C_4H_9)_4N$]-OH was used instead of KOH to deprotonate the ligand. Diffraction quality crystals were obtained by slow evaporation at 5 °C of a THF/$CHCl_3$ solution of [$(C_4H_9)_4N$][V^VO(HIBA)].

[$V^{IV}O$(HIBA)]$^{2-}$. The vanadium(IV) complex of $HIBA^{4-}$ was prepared by dissolution of $VO(acac)_2$ (1 equiv), H_4HIBA (1 equiv), and KOH (4 equiv) in CH_3CN under N_2 in a Vacuum Atmospheres inert atmosphere box. The green reaction mixture was stirred for 30 min. and allowed to settle. The supernatant was separated by filtration, and the solvent was removed under vacuum to yield a green solid. EPR measurements were obtained on DMF/EtOH (9:1 v/v) solutions of this solid.

(11) (a) Rehder, D.; Weidemann, C.; Duch, A.; Priebsch, W. *Inorg. Chem.* **1988**, *27*, 584−587. (b) Rehder, D. *Inorg. Chem.* **1988**, *27*, 4312−4316.
(12) Kabanos, T. A.; Keramidas, A. D.; Papaioannou, A. B.; Terziz, A., *J. Chem. Soc., Chem. Commun.* **1993**, 643−645.
(13) Cornman, C. R.; Geiser-Bush, K. M.; Singh, P. *Inorg. Chem.* **1994**, *33*, 4621−4622.
(14) Hanson, G. R.; Kabanos, T. A.; Keramidas, A. D.; Mentzafos, D.; Terzis, A. *Inorg. Chem.* **1992**, *31*, 2587−2594.
(15) Borovik, A. S.; Dewey, T. M.; Raymond, K. N. *Inorg. Chem.* **1993**, *32*, 413−421.
(16) Chasteen, N. D. In *Biological Magnetic Resonance*; Berliner, L. J., Reuben, J., eds.; Plenum Press; New York, 1981; Vol. 3, pp 53−119.
(17) Eaton, S. S.; Eaton, G. R. In *Vanadium in Biological Systems*; Chasteen, N. D.; Ed.; Kluwer Academic Publishers: Dordrecht, The Netherlands 1990; pp 199−222.
(18) $A_i = A/4$ as described in reference 16.
(19) Cornman, C. R.; Geiser-Bush, K. M. Unpublished Results. We have compared A_z for $V^{IV}O$(SALEN) and the bis(Schiff base) complex $V^{IV}O$(*N*-methyl-salicylideneamine)$_2$ in frozen toluene solution. Despite significant structural differences (determined by X-ray crystallography), the difference in $A_z = \pm 1 \times 10^{-4}$ cm^{-1}.
(20) It has been shown that vanadyl complexes of bidentate Schiff-base ligands can be distorted away from square pyramidal geometry toward trigonal bipyramidal geometry. Mazzanti, M.; Floriani, C.; Chiesi-Villa, A.; Guastini, C. *J. Chem. Soc. Dalton Trans.* **1989**, 1793−1798.
(21) Anson, F. C.; Collins, T. J.; Richmond, T. G.; Santarsiero, B. D.; Toth, J. E.; Treco, G. R. T. *J. Am. Chem. Soc.* **1987**, *109*, 2974−2979.
(22) Barnes, D. J.; Vagg, C. R. S.; Watton, E. C. *J. Chem. Eng. Data* **1978**, *23*, 349−350.

Table 1. Summary of Crystallographic Data for $V^{IV}O$(PAIS) and $[V^{V}O(HIBA)][N(C_4H_9)_4]$

	$V^{IV}O$(PAIS)	$[V^{V}O(HIBA)][N(C_4H_9)_4]$
formula	$C_{19}H_{13}N_3O_3V$	$C_{30}H_{52}N_3O_5V$
mol wt	382.08	585.69
$F(000)$	779.85	1265.54
cryst syst	monoclinic	monoclinic
space group	$P2_1/n$	$P2_1/n$
a, Å	7.777(3)	13.228(3)
b, Å	18.433(7)	16.054(4)
c, Å	11.676(4)	14.7140(20)
β, deg	102.66(3)	93.240(10)
V, Å^3	1633(1)	3119.7(11)
d_{calc}, g/cm^3	1.55	1.247
Z	4	4
radiation	Mo Kα (0.7107 Å)	
temp, °C	ambient	-143
abs coeff, mm^{-1}	0.66	0.35
cryst size, mm	0.45 × 0.40 × 0.35	0.50 × 0.50 × 0.35
cryst color	brown	brown/green
scan speed, deg/min	0.5− 24.0	2
scan range, deg	$3 < 2\theta < 50$	$3 < 2\theta < 46.1$
no. of unique data	2870	4362
no. of obsd data	1612 (F_o) ≥ 5σ(F)	3885 (F_o) > 1σ(F)
octants used	hkl, (−h)kl	hkl, (−h)kl
residual elect dens, e/Å^3	+0.52/−0.36	+0.270/−0.38
R^a	0.0600	0.051
$R_w{}^b$	0.0450	0.047
GoF	1.410	1.33

^{a} $R = \Sigma(|F_o - F_c|)/(\Sigma|F_o|)$. ^{b} $R_w = [\Sigma(w|F_o - F_c|)^2/\Sigma w(F_o)^2]^{1/2}$.

Table 2. Atomic Coordinates and Isotropic Thermal Parameters (Å × 10^3) for $V^{IV}O$(PAIS)

	x	y	z	U^a
V	0.0617(1)	0.9749(1)	0.2276(1)	40(1)
C1	0.0461(7)	1.1269(3)	0.1634(4)	41(2)
C2	0.0009(7)	1.1777(3)	0.0711(4)	50(2)
C3	0.0754(8)	1.2456(3)	0.0821(5)	57(2)
C4	0.1951(8)	1.2659(3)	0.1819(5)	61(3)
C5	0.2380(7)	1.2190(3)	0.2734(4)	54(2)
C6	0.1689(7)	1.1482(3)	0.2665(4)	40(2)
C7	0.2203(7)	1.1019(3)	0.3683(4)	44(2)
N1	0.1835(5)	1.0339(2)	0.3708(3)	40(2)
C8	0.2306(7)	0.9913(3)	0.4770(4)	40(2)
C9	0.3483(7)	1.0111(3)	0.5782(4)	46(2)
C10	0.3850(7)	0.9646(4)	0.6730(5)	54(3)
C11	0.3030(7)	0.8983(3)	0.6652(5)	55(2)
C12	0.1844(7)	0.8769(3)	0.5643(4)	48(2)
C13	0.1435(6)	0.9243(3)	0.4683(4)	40(2)
N2	0.0291(5)	0.9119(2)	0.3595(3)	41(2)
C14	−0.0975(7)	0.8601(3)	0.3396(5)	47(2)
O1	−0.1309(5)	0.8136(2)	0.4090(3)	62(2)
C15	−0.2109(7)	0.8650(3)	0.2165(4)	40(2)
C16	−0.3515(8)	0.8207(3)	0.1766(5)	51(2)
C17	−0.4563(7)	0.8327(3)	0.0664(5)	63(3)
C18	−0.4181(8)	0.8896(3)	0.0017(5)	66(3)
C19	−0.2755(8)	0.9325(3)	0.0450(5)	53(3)
N3	−0.1705(5)	0.9205(2)	0.1512(3)	41(2)
O2	−0.0297(4)	1.0620(2)	0.1503(3)	48(1)
O3	0.2158(5)	0.9438(2)	0.1720(3)	54(2)

^{a} Equivalent isotropic U defined as one-third of the trace of the orthogonalized $\mathbf{U}_{ij}$ tensor.

Collection and Reduction of X-ray Data. Suitable crystals of $V^{IV}O$(PAIS) and $[V^{V}O(HIBA)][N(C_4H_9)_4]$ were obtained as described above. Crystal and data acquisition parameters are given in Table 1. Fractional atomic coordinates for $V^{IV}O$(PAIS) and the anion of $[V^{V}O(HIBA)][N(C_4H_9)_4]$ are given in Tables 2 and 3, respectively. Selected bond distances and angles for these compounds are provided in Table 4. $V^{IV}O$(PAIS) was mounted on a glass fiber with epoxy. Intensity data were obtained at room temperature on a Siemens R3/μ diffractometer using Mo Kα radiation (0.7107 Å). Three standard reflections were measured every 97 reflections. Intensity data were collected using $\theta/2\theta$ scans. The data were reduced and the structure was solved and refined using the Siemens SHELXTL PLUS program package implemented on a Data General Microeclipse computer. In the subsequent refinement, the function $\Sigma w(|F_o| - |F_c|)^2$ was minimized using block-diagonalized least-squares methods (F_o and F_c are the observed and calculated structure factor amplitudes). Atomic scattering factors are taken from ref. 23. Unique data and final R indices are reported in Table 1.

Table 3. Atomic Coordinates and B_{iso} for the Anion of $[V^{V}O(HIBA)][(C_4H_9)_4N]$

	x	y	z	$B_{iso}{}^a$
V	0.38021(3)	0.25769(3)	0.24825(3)	1.739(21)
O1	0.29870(14)	0.32969(14)	0.22808(13)	2.72(10)
O2	0.52494(15)	0.29732(13)	0.49700(12)	2.43(9)
O3	0.34419(15)	0.20113(13)	0.34708(12)	2.55(9)
O4	0.37212(15)	0.18390(12)	0.15619(12)	2.28(8)
O5	0.55121(17)	0.29149(14)	0.02981(13)	3.30(10)
N1	0.48092(16)	0.30176(13)	0.34197(14)	1.48(9)
N2	0.49450(16)	0.29651(14)	0.17546(14)	1.53(9)
C1	0.56915(20)	0.34750(16)	0.21797(17)	1.52(11)
C2	0.64913(21)	0.38653(18)	0.17828(21)	1.87(12)
C3	0.72018(23)	0.42846(19)	0.23321(22)	2.33(14)
C4	0.71189(23)	0.43300(19)	0.32611(22)	2.32(13)
C5	0.63154(22)	0.39498(17)	0.36678(20)	1.92(13)
C6	0.56147(19)	0.35100(16)	0.31318(17)	1.34(10)
C7	0.47573(21)	0.27358(17)	0.42903(18)	1.70(11)
C8	0.40163(21)	0.20069(18)	0.43208(17)	1.87(12)
C9	0.4626(3)	0.12105(21)	0.4416(3)	2.92(16)
C10	0.3306(3)	0.20930(22)	0.50911(20)	2.04(13)
C11	0.41881(22)	0.19759(19)	0.07261(18)	2.29(13)
C12	0.3397(3)	0.2244(3)	0.0003(3)	3.54(17)
C13	0.4723(3)	0.1184(3)	0.0470(3)	3.49(17)
C14	0.49616(22)	0.26727(18)	0.08905(18)	2.07(12)

^{a} B_{iso} is the mean of the principle axes of the thermal ellipsoid. $B_{iso} = (8\pi^2)U_{iso}$.

Table 4. Important Bond Lengths (Å) and Angles (deg) for $V^{IV}O$(PAIS) and $[V^{V}O(HIBA)][N(C_4H_9)_4]$

	$V^{IV}O$(PAIS)		
V−O2	1.901(3)	V−N2	1.989(4)
V−O3	1.590(3)	V−N3	2.087(4)
V−N1	2.045(4)		
O3−V−O2	110.3(2)	N1−V−O2	89.7(1)
O3−V−N1	105.6(2)	N1−V−N3	143.9(2)
O3−V−N2	109.9(2)	N2−V−N3	78.7(2)
O3−V−N3	108.1(2)	N2−V−O2	139.7(2)
N1−V−N2	78.2(2)	N3−V−O2	90.3(1)
	$[V^{V}O(HIBA)][N(C_4H_9)_4]$		
V−O1	1.5971(21)	V−N1	1.9924(22)
V−O3	1.8012(19)	V−N2	2.0010(21)
V−O4	1.7981(19)		
O1−V−O3	107.95(10)	O3−V−N2	146.24(9)
O1−V−O4	109.03(10)	O3−V−O4	105.60(9)
O1−V−N1	106.83(10)	N1−V−N2	76.35(9)
O1−V−N2	101.40(10)	N1−V−O4	139.85(9)
O3−V−N1	79.47(9)	N2−V−O4	79.43(9)

$[(C_4H_9)_4N][V^{V}O(HIBA)]$ was mounted on a glass fiber in the cold stream of a Rigaku AFC 6S diffractometer using silicon grease. The diffractometer was controlled using the program DIFRAC.[24] Intensity data were obtained at 130 K using Mo Kα radiation (0.7107 Å). Three standard reflections were measured every 100 reflections. Intensity data were collected using ω scans. An empirical absorption correction was carried out using ψ scan data. The data were reduced and refined using the NRCVAX suite of programs.[25] The structure was solved

(23) *International Tables for X-ray Crystallography*; Ibers, J., Hamilton, W., Eds.; Kynoch: Birmingham, England, 1974; Vol. IV, Tables 2.2 and 2.3.1.
(24) Gabe, E. J.; White, P. S. Presented at the American Crystallographic Association Annual Meeting, Atlanta, GA, 1994; Abstract M14.
(25) Gabe, E. J.; Le Page, Y.; Charland, J.-P.; Lee, F. L.; White, P. S. *J. Appl. Crystallogr.* **1989**, *22*, 384−387.

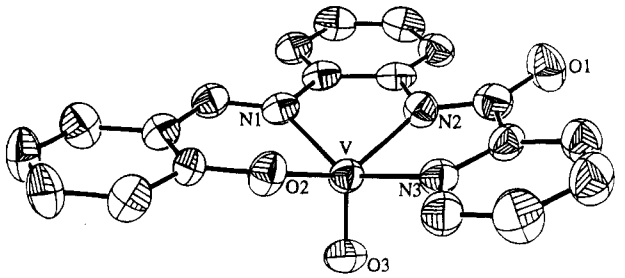

Figure 1. Perspective veiw of $V^{IV}O$(PAIS). Thermal ellipsoids are at 50% probability.

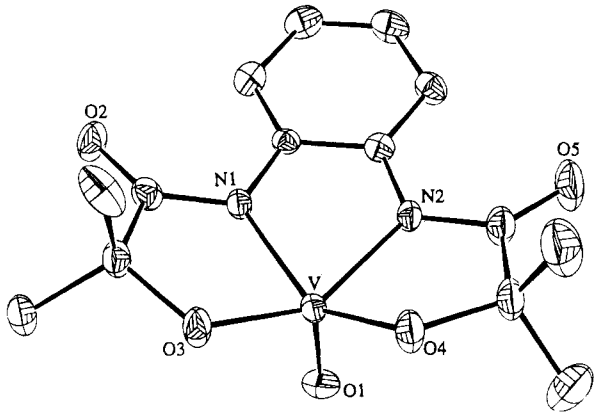

Figure 2. Perspective veiw of the anion of $[V^{V}O(HIBA)][(C_4H_9)_4N]$. Thermal ellipsoids are at 50% probability.

using the program SIR92.[26] Non-hydrogen atoms were refined using anisotropic displacement parameters. All hydrogen atoms were located on difference Fourier maps and were allowed to refine isotropically. The function $\Sigma w(|F_o| - |F_c|)^2$ was minimized using full-matrix least-squares methods. Unique data and final R indices are reported in Table 1.

Spectroscopic Measurements. Infrared spectra were obtained using a Mattson Polaris FTIR spectrometer. Electron paramagnetic resonance measurements were obtained using an IBM ER200D instrument with a TE_{102} cavity and a quartz finger dewar. The spectra were collected on 1−5 mM DMF/EtOH (9:1 v/v) solutions at 77 K (liquid nitrogen). Microwave frequencies in the 9.5 GHz range were calibrated using DPPH (g = 2.0037) and the magnetic field provided by the ER 031M field controller. The $5G_{pp}$ modulation and gain $\approx 5 \times 10^4$ were typical. Spin Hamiltonian parameters were determined using the simulation program QPOW.[27] The samples for $V^{IV}O$(PAAP) invariably contained some organic radical signal which was subtracted from the raw data prior to the spectral fit. Figures 10, 11, and 12 showing this data and the spectral fits are included in the supporting information.

Results and Discussion

Structural Studies. $V^{IV}O$(PAIS) and $[V^{V}O(HIBA)][N(C_4H_9)_4]$ have been crystallographically characterized and their molecular structures are presented in Figures 1 and 2, respectively. Parametrical data are provided in Table 4. The $V^{IV}O$(PAIS) structure consists of an equatorial tetradentate ligand that provides pyridyl, amido, imino and phenolato coordination to the V=O group. The overall geometry is best described as a distorted square pyramid based on idealized polytopal forms.[28] The angle between the basal planes containing O2, N1, and N3 and N1, N2, and N3 is 173.5° (180° expected for a pure square pyramidal complex). The $V-N_{amido}$ bond distance of 1.990(4) Å suggests that the amide nitrogen is a slightly better donor than imine nitrogen donor ($V-N_{imino}$ = 2.047(4) Å) in this complex. The $V-N_{amido}$ distances reported to date are in the range 1.970−2.026 Å and are, in general, slightly shorter than $V^{IV}-N_{imino}$. The amido moiety [−C−(C=O)−N−C−] of the ligand in $V^{IV}O$(PAIS) (as well as the other reported vanadium−amido complexes) is planar indicating significant conjugation within this unit. This observation also supports the proposed deprotonated nature of this ligand. Collins has interpreted deviations from planarity of the amido unit as indicating a decrease in the conjugation making the nitrogen lone pair available for π-bonding to the metal atom.[29] This does not seem to be occurring with the vanadium−amide complexes examined to date. The vanadium atom sits 0.63 Å out of the best plane defined by O2, N1, N2, and N3 as expected for a five-coordinate, square pyramidal complex.

$[V^{V}O(HIBA)]^-$ is the first structurally characterized vanadium(V) complex containing a vanadium(V)−N_{amide} bond. A preliminary structural report of the potassium salt of this complex has been published.[13] In that report, the crystals of $K[V^{V}O(HIBA)]$ contained an additional H_4HIBA ligand. The structure of the tetrabutyl ammonium salt reported here does not contain this additional ligand; however, the metal coordination environment remains quite similar. The first coordination sphere consists of an oxo donor (1.5971(21) Å), two alkoxide oxygen donors (1.8012(19), 1.7981(19) Å) and two deprotonated amide−nitrogen donors (1.9924(22), 2.0010(21) Å). Again, the overall geometry is best described as a distorted square pyramid with an angle between the basal planes (containing O4, N1, and N2 and O4, O3, and N1) of 174.7°. The vanadium sits 0.58 Å out of the best plane defined by O3, O4, N1, and N2. One might expect the d^0 vanadium(V)−HIBA complex to have shorter metal−ligand distances than those observed in the previously reported vanadium(III or IV)−amide structures (range = 1.970(2) − 2.026(6) Å; mean = 1.996 Å). That this is not the case ($V-N_{amide} \approx$ 1.9969 Å is the average of the reported values) is due to the strong, trans-coordinated alkoxide donors. The planarity of the amide moiety confirms the deprotonated nature of the amide nitrogen atom. The vanadium−alkoxide distances are slightly longer than most other vanadium(V)−alkoxide structures reported in the literature.[30] Kabanos and coworkers have recently reported the structure of a six-coordinate vanadium(V)−amide complex in which the amide oxygen, and not the amide nitrogen, is coordinated to the metal ion in the position trans to the oxo ligand.[31]

The complex $V^{IV}O$(PAAP) is assumed to be isostructural with $V^{IV}O$(PAIS) and $[V^{V}O(HIBA)]^-$ in solution. The complex $[Fe^{III}(PAAP)(Cl)_2][Et_3HN]$ has been crystallographically characterized and demonstrates the preferred planar coordination mode for this ligand.[32] Infrared spectroscopic studies of KBr pellets suggest an oxo-bridged linear chain motif in the solid state (Figure 3). Vanadium−oxo (V=O) stretching frequencies

(26) Program SIR92, Altomare, A.; Cascarano, G.; Giacovazzo, C.; Guagliardi, A., Ist. di Ric. per lo Sviluppo di Metodologie Cristallografiche, CNR, c/o Dip. Geomineralogico−Univ. of Bari; Burla, M. C.; Polidori, G., Dip. Scienze della Terra−Univ. of Perugia; Camalli, M., Ist. Strutt. Chimica CNR, Monterotondo stazione−Rome.

(27) Program QPOW by R. L. Belford, A. M. Maurice, and J. M. Nilges: (a) Nilges, M. J., Ph.D Thesis, University of Illinois, Urbana, IL, 1979, (b) Belford, R. L.; Nilges, M. J., Computer Simulation of Powder Spectra. Presented at the EPR Symposium, 21st Rocky Mountain Conference, Denver, CO, August, 1979, (c) Maurice, A. M. Ph.D. Thesis, University of Illinois, Urbana, IL, 1980.

(28) Muetterties, E. L.; Guggenberger, L. J. *J. Am. Chem. Soc.* **1974**, *96*, 1748−1756.

(29) Collins, T. J.; Coots, R. J.; Furutani, T. T.; Keech, J. T.; Peake, G. T.; Santarsiero, B. D. *J. Am. Chem. Soc.* **1986**, *108*, 5333−5339.

(30) Carrano, C. J.; Mohan, M.; Holmes, S. M.; de la Rosa, R.; Butler, A.; Charnock, J. M.; Garner, C. D. *Inorg. Chem.* **1994**, *33*, 646−655.

(31) Kabanos, T. A.; Keramidas, A. D.; Papaioannou, A.; Terzis, A. *Inorg. Chem.* **1994**, *33*, 845−846.

(32) Yang, Y.; Diedrich, F.; Valentine, J. S. *J. Am. Chem. Soc.* **1991**, *113*, 7195−7205.

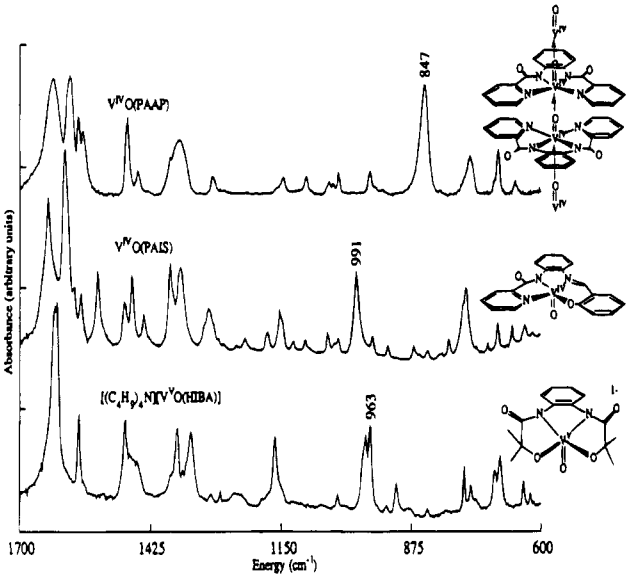

Figure 3. FTIR spectra of $V^{IV}O$(PAAP) (top), $V^{IV}O$(PAIS) (center), and $[V^{V}O(HIBA)][(C_4H_9)_4N]$ (bottom). V=O stretching frequencies are labeled.

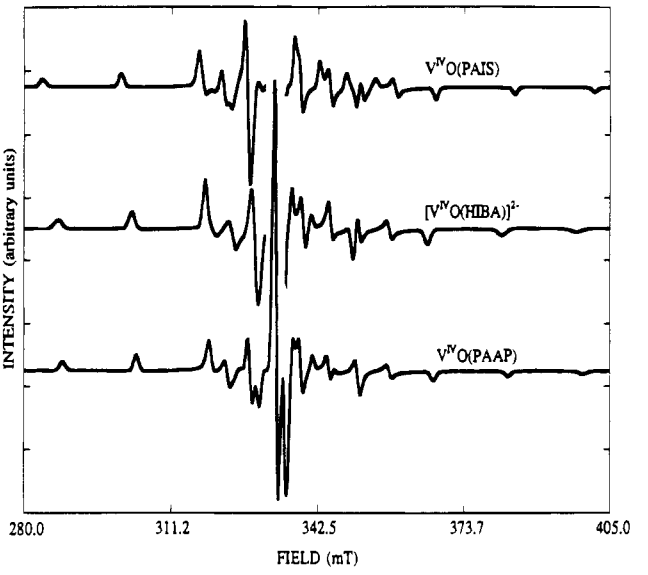

Figure 4. EPR spectra of $V^{IV}O$(PAIS) (top), $[V^{IV}O(HIBA)]^{2-}$ (center), and $V^{IV}O$(PAAP) (bottom).

are normally intense absorptions[33] between 900 and 1000 cm^{-1} and are observed at 991 and 963 cm^{-1} for $V^{IV}O$(PAIS) and $[V^{V}O(HIBA)][N(C_4H_9)_4]$, respectively.[34] The corresponding band for $V^{IV}O$(PAAP) has a frequency of 847 cm^{-1}. This low value for $\nu_{V=O}$ is similar to those observed for $V^{IV}O$(salpn) (854 cm^{-1}; salpn is the Schiff base formed between salicylaldehyde and 1,3-diaminopropane), a complex that forms an oxo-bridged linear chain (→V=O→V=O→V=O→) in the solid state[35] and, $[V(^{-}SNNS^{-})]_4(\mu\text{-}O)_4$ (874 cm^{-1}, $^{-}SNNS^{-}$ is the dianion of *N,N'*-bis(*o*-mercaptophenyl)ethylenediamine) which forms four bent V=O→V linkages.[36] The low stretching frequency for bis[*N*-(4-chlorophenyl)salicylideneaminato]oxovanadium(IV) (888 cm^{-1})[20] has been discussed in a similar context.[37] These low stretching frequencies are thus associated with donation of π-electrons from one V=O unit to the next vanadium atom in the chain, thus decreasing the V=O bond order. Additionally, a structural trans influence may contribute to this low frequency.[38]

Amide Contribution to A_z. The EPR spectra for $V^{IV}O$(PAAP), $V^{IV}O$(PAIS), and $[V^{IV}O(HIBA)]^{2-}$, as frozen DMF/EtOH (9:1 vol/vol) solutions are presented in Figure 4. Spin Hamiltonian parameters are provided in Table 5. Using eq 1 and the values for $A_{z,i}$ also provided in Table 5 (for ArO^{-}, RO^{-}, "aliphatic" amine, and "aromatic" imine), the calculated values for $A_{z,amide}$ are between 31 × 10^{-4} and 37 × 10^{-4} cm^{-1} (including two values for two amide complexes from the literature, ref 14).[39] The average value for $A_{z,amide}$ is 34 × 10^{-4} cm^{-1}, which is much lower than that of other nitrogen ligands. Indeed, the value for deprotonated amide nitrogen approaches that of a thiolate sulfur, $A_{z,RS^-} = 32 \times 10^{-4}$ cm^{-1}. Thus, the deprotonated amide nitrogen places a significant amount of electron density on the metal center, decreasing the interaction between the metal centered unpaired electron (d_{xy}^1) and the vanadium nuclear spin. Since the EPR data for $V^{IV}O$(pycac) and $V^{IV}O$(pycbac) were collected in CH_2Cl_2,[14] the value for $A_{z,amide}$ appears to be insensitive to the solvent for the neutral complexes.

The large range of amide contributions, 31 × 10^{-4} to 37 × 10^{-4} cm^{-1}, suggests that the amide contribution is sensitive to the balance of the coordination sphere. This may reflect the electron distribution within the amide unit since $A_{||}$ increases with decreasing donation of electron density from the ligands. As shown in Figure 5, electron delocalization from the amide *nitrogen* (resonance form **A**, small contribution to A_z) out to the amide *oxygen* (resonance form **C**, larger contribution to A_z) to maintain electroneutrality at the metal center may be responsible for this difference. Accordingly, the amide unit becomes more "imine-like" ($A_{z,imine} = 44.4 \times 10^{-4}$ cm^{-1}, Table 5) as the equatorial coordination sphere becomes more anionic. Note that this suggests that the amide group in $V^{IV}O(HIBA)^{2-}$ is more "pyridyl-like" ($A_{z,pyridyl} = 38.3 \times 10^{-4}$ cm^{-1}, Table 5).

Serum albumin[40] and bleomycin[41] both bind metal ions using deprotonated amide nitrogens. By analogy to other metal complexes, the vanadyl-bleomycin and albumin structures shown in Figure 6 might be expected.[32,33] Bleomycin utilizes an imidazole nitrogen, a secondary amine, a pyrimidine nitrogen, and a deprotonated amide nitrogen to coordinate to the equatorial sites of metal ions. Since the proposed amide nitrogen ligand is the only negatively charged ligand in the equatorial coordination sphere, one would expect the electronic distribution in the amide unit to be dominated by resonance structure **A** in Figure 5. For vanadyl–bleomycin the experimental[7] $A_z = 154.5 \times 10^{-4}$ cm^{-1} which is in good agreement with the value calculated from eq 1, $A_{z,calcd} = 154 \times 10^{-4}$ cm^{-1}, using $A_{z,amide} = 32 \times 10^{-4}$ cm^{-1} (structure **A**, Figure 5).

For serum albumin, the proposed Cu^{II} and Ni^{II} binding site is at the N-terminus and uses the N-terminal amine, two deprotonated amide nitrogens, and an imidazole nitrogen as

(33) (a) Selbin, J. *Coord. Chem. Rev.* **1966**, *1*, 293–314. (b) Selbin, J.; Holmes, L. H. Jr.; McGlynn, S. P. *J. Inorg. Nucl. Chem.* **1963**, *25*, 1359–1369.
(34) Of the two signals present at ≈980 cm^{-1} in the infrared spectrum of $[VVO(HIBA)][N(C_4H_9)_4]$, the one at higher energy is also present in the spectrum of the free ligand and in the spectrum of the tetrabutyl ammonium cation. Thus, this signal has been attributed to a ligand or cation vibration.
(35) Mathew, M.; Carty, A.; Palenik, G. J. *J. Am. Chem. Soc.* **1970**, *92*, 3197–3198.
(36) Tsagkalidis, W.; Rodewald, D.; Rehder, D. *Inorg. Chem.* **1995**, *34*, 1943–1945.
(37) Hamilton, D. E. *Inorg. Chem.* **1991**, *30*, 1670–1671.
(38) Scheidt, R. W. *Inorg. Chem.* **1973**, *12*, 1758–1761.
(39) For instance, for $V^{IV}O$(PAIS): (all × 10^{-4} cm^{-1}) A_z(amide) = 154 − 38.3 − 44.4 − 38.6 = 33.
(40) Laussac, J.-P.; Sarkar, B. *Biochemistry* **1984**, *23*, 2832–2838.
(41) Guajardo, R. J.; Hudson, S. E.; Brown, S. J.; Mascharak, P. K. *J. Am. Chem. Soc.* **1993**, *115*, 7971–7977.

Table 5. EPR Parameters for Use in Eq 1 and Experimental Parameters for $V^{IV}O$(PAAP), $V^{IV}O$(PAIS), and $K_2[V^{IV}O$(HIBA)

compound	$g_\perp$	$g_\parallel$	$A_\perp$,[a] 10^4 cm^{-1}	$A_\parallel$, 10^4 cm^{-1}	$A_{z,i}$,[b,c] 10^4 cm^{-1}
H_2O	1.980	1.933	68.2	182.6	45.7
=N−			54.9	177.6	44.4
("aliphatic" imine)					
Ar−CO_2^-	1.979	1.941		170.9	42.7
R−CO_2^-	1.08	1.941		170.9	42.7
=N−			57.3	153.2	38.3
("aromatic" imine)					
R−NH_2	1.979	1.955		160.3	40.1
Ar−O^-			56.1	154.4	38.6
OH^-	1.977	1.982		154.7	38.7
=C−O^-			55.1	150.4	37.6
(acac type −O^-)					
Ar−S^-	1.988	1.982		141.7	35.3
R−O^-	1.985	1.967		141.3	35.3
R−S^-	1.987	1.987		127.7	31.9
$V^{IV}O$(PAAP)	1.982	1.954	49	143	35[d]
	$g_x = 1.983$	$g_z = 1.955$	$A_x = 51$	$A_z = 145$	
	$g_y = 1.988$		$A_y = 37$		
$V^{IV}O$(PAIS)	$g_x = 1.986$	$g_z = 1.961$	$A_x = 45$	$A_z = 154$	33[d]
	$g_y = 1.982$		$A_y = 54$		
$[V^{IV}O$(HIBA)$]^{2-}$	$g_x = 1.979$	$g_z = 1.964$	$A_x = 50$	$A_z = 145$	37[d]
	$g_y = 1.989$		$A_y = 35$		
$V^{IV}O$(pycac)[e]	$g_x = 1.978$	$g_z = 1.956$	$A_x = 53.6$	$A_z = 151.4$	31[d]
	$g_y = 1.981$		$A_y = 42.5$		
$V^{IV}O$(pycbac)[e]	$g_x = 1.976$	$g_z = 1.957$	$A_x = 53.6$	$A_z = 152.4$	32[d]
	$g_y = 1.981$		$A_y = 38.3$		
vanadyl−albumin	1.979	1.939	64.0	172.8	see text
vanadyl−bleomycin	1.990	1.966	53.0	152.6	see text

[a] $A_\perp = 0.5(A_x + A_y)$. [b] $A_{z,i}$ is defined as the z component of the isolated contribution to the coupling constant. This is equivalent to $A_{\parallel,i}$ in axial symmetry (see text, eq 1). [c] Values for $A_{z,i}$ are from ref 16. The values for Ar−O^- were derived from VO(salycilate)$_2$ and Ar−CO_2^-. The value for "aromatic" imine were derived from VO(picolinate)$_2$ and Ar−CO_2^-. The value for =C−O^- derived from VO(acacen) and "aliphatic" imine. [d] $A_{z,\text{amide}}$ from the present work. [e] From ref 14.

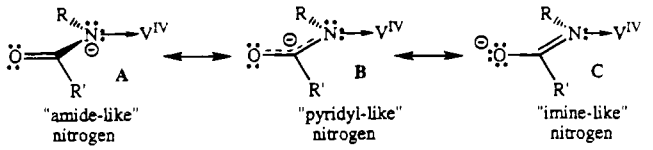

Figure 5. Resonance structures for amide ligand coordinated through the nitrogen.

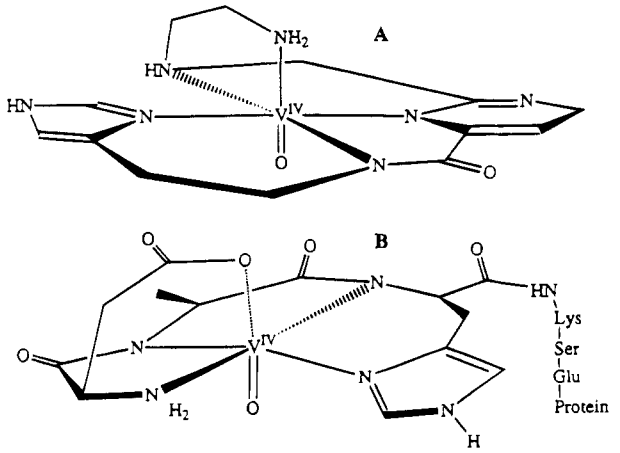

Figure 6. Possible structures for the active site of vanadyl−bleomycin, **A**, and vanadyl−serum albumin, **B**.

metal equatorial ligands. Considering that the balance of the proposed equatorial coordination sphere consists of neutral donors, one would again expect resonance structure **A** (Figure 5) to dominate the electronic structure of the amide unit. For vanadyl-serum albumin the experimental[10] $A_z = 172.8 \times 10^{-4}$ cm^{-1} which does not agree with the value calculated from eq 1, $A_{z,\text{calcd}} = 145 \times 10^{-4}$ cm^{-1} (again, using $A_{z,\text{amide}} = 32 \times 10^{-4}$cm^{-1}, resonance structure **A**, Figure 5). The difference of 28×10^{-4} cm^{-1} between the experimental and calculated parallel coupling constants suggests that deprotonated amide nitrogens are *not* coordinated to the vanadyl ion. A smaller discrepancy was noted by Chasteen and Fracavilla and led them also to conclude that amide nitrogens are *not* involved in vanadyl coordination in serum albumin.[10]

Two alternative possibilities are quite plausible for the vanadyl binding site of serum albumin. The first consists of a carboxylate from Asp-1, an imidazole nitrogen from His-3, and two water ligands (or a water and the terminal amine) and yields $A_{z,\text{calc}} \approx 175 \times 10^{-4}$ cm^{-1}. The second consists of an imidazole nitrogen from His-3, alcohol oxygen from Ser-5 (or water), carboxylate oxygen from Glu-6 and a water ligand. This combination of equatorial ligands yields $A_{z,\text{calc}} \approx 172 \times 10^{-4}$ cm^{-1}.

To date, vanadium(IV) complexes of aliphatic amides, which would provide a better biological model, have not been isolated (work in progress). This may reflect the inherent instability of these complexes. However, in the absence of these data, one can predict that $A_{z,i}$ for a deprotonated aliphatic amide will be lower than those for the aromatic amides shown above. As indicated in Table 5, aliphatic alcohols and thiols have lower values for $A_{z,i}$ than their aromatic counterparts. A similar trend is expected to hold for aliphatic amides.

Conclusion

The contribution of a deprotonated amide nitrogen to A_z, based on the additivity relationship (eq 1) has been determined. Comparison of calculated and experimental values for $A_\parallel$ may be used to support the presence or absence of a ligand within a proposed coordination environment. For the two vanadyl−amide biomolecules considered, this analysis supports the presence of a deprotonated amide ligand for vanadyl−bleomycin while suggesting that deprotonated amide ligands are not present

in vanadyl–albumin. The identity of the coordinating ligands in vanadyl–albumin will affect the properties of the vanadium that is delivered to cells, proteins, and co-factors. Additionally, the similarity of A_{z,RS^-} and $A_{z,amide}$ requires that amide coordination be considered when examining the EPR spectra of cysteine containing polypeptides or proteins; i.e., a low coupling constant is not definitive evidence for thiolate coordination. This may prove important given the vanadium inhibition of protein tyrosine phosphatases which are involved in the insulin induced phosphate cascade and contain a cysteine at their active site.

Acknowledgment. Financial support from the Department of Chemistry, North Carolina State University is gratefully acknowledged. The authors wish to thank Dr. Peter White of the Department of Chemistry, University of North Carolina at Chapel Hill, for his assistance in collecting the X-ray data for $[V^{V}O(HIBA)][(C_4H_9)_4N]$.

Supporting Information Available: For $V^{IV}O(PAIS)$, Tables 6–10 listing atomic coordinates, thermal parameters, a complete set of bond distances and a complete set of bond angles, Figure 7 providing a full numbering scheme for $V^{IV}O(PAIS)$, for $[V^{IV}O(HIBA)][(C_4H_9)_4N)]$, Tables 12–15 listing atomic coordinates, thermal parameters, a complete set of bond distances, and a complete set of bond angles, Figure 8 providing complete numbering scheme for the anion of $[V^{IV}O(HIBA)][(C_4H_9)_4N)]$, Figure 9 providing complete numbering scheme for the cation of $[V^{IV}O(HIBA)][(C_4H_9)_4N)]$, and Figures 10–12 show the QPOW fits of the EPR data for VOPAIS, VO(PAAP), and $VO(HIBA)^{2-}$, repectively (19 pages). Ordering information given on any current masthead page.

IC941414U